Hypothesis on the karstification/dolomitization of the Barremian reservoir in Parentis Basin

Alexandre Ortiz, Aloys Baudesson, Christine Flehoc, Catherine Guerrot, Xavier Lopez, Olivier Douez, Gabrielle Rumbach

Short Papers from the 19th French Congress of Sedimentology, Lille, 2024.
ASF Publ. n°84. CC-BY © 2025 The Authors
Article DOI: 10.70655/VYWM6440

HYPOTHESIS ON THE KARSTIFICATION/DOLOMITIZATION OF THE BARREMIAN RESERVOIR IN PARENTIS BASIN

Alexandre ORTIZ[1], Aloys BAUDESSON[2], Christine FLEHOC[1], Catherine GUERROT[1], Xavier LOPEZ[2], Olivier DOUEZ[1], Gabrielle RUMBACH[2,3],

[1]*BRGM – Bureau de Recherches Géologiques et Minières*
[2]*Vermilion-Rep SAS*
[3]*ES-Geothermie*

Corresponding author: a.ortiz@brgm.fr

Abstract: The Parentis sub-Basin, located southwest of Bordeaux (France), has been known since the 1950s as a prolific oil reservoir. It lies at the eastern end of the Bay of Biscay. Several fields are exploited in the onshore part of the basin, the largest being at Parentis-en-Born, discovered by ESSOREP in 1954 and exploited by VERMILION REP since 2006. The field is an east-west anticlinal structure, formed during various geodynamic episodes in connection with halokinesis of the Triassic and Hettangian series. One of the reservoirs exploited is a limestone/dolomite dating from the Barremian to the Upper Jurassic characterized by a matrix porosity of 14% and a permeability of 100 mD over an average thickness of 200 metres.

Numerous studies and acquisitions (3D seismic, 122 boreholes) have been carried out by ESSOREP and VERMILION REP exploration geologists to characterise the limestone/dolomite reservoir, particularly regarding the origin of the dolomitization and porosity. Models of emplacement suggest post-sedimentary dolomitization by reflux and epigenic karstification linked to early tectonic bulges.

Our study aims to use modern methods and concepts to gain a better understanding of the major stages in the development of this reservoir in relation to the geodynamic events. It is based on a detailed study of cores and thin sections. A total of 160 samples were taken from 7 boreholes to conduct a diagenetic study (petrography, cathodoluminescence and initial results on strontium isotopes).

The macroscopic study of the cores showed the presence of numerous mud losses (no-recovery zones), often correlated with faults (striations observed), which were previously interpreted as epigenic karstification. Numerous veins were observed in the fracture zones, composed of calcite, saddle dolomite and anhydrite. Microscopically, the paragenesis shows primary dolomitization prior to burial (euhedral to subhedral dolomite), followed by phases of circulation of magnesium-rich hydrothermal fluids (saddle dolomite - 'non-planar') and sulphates (anhydrite).

Initial interpretations suggest that the void zones encountered in the boreholes are linked to the upwelling of deep-seated fluids sourced by Triassic/Lower Jurassic evaporites and dolomites, resulting in hypogenic karstification. These episodes would be linked to the resumption of the anticline during the Pyrenean phase.

Keywords: Aquitaine Basin, parentis, hypogene, thin-section, saddle dolomite.

1 INTRODUCTION

The Parentis sub-basin is the eastern termination of the V-shaped bay of Biscay and recorded several structuration phases related to geodynamic events, (i) an initial phase of Permian-Triassic rifting culminated in the deposition of thick Keuper evaporites (Bourrouilh et al., 1995; Brunet, 1994; Desegaulx and Brunet, 1990; Mathieu, 1986), (ii) a second rifting phase took place between the latest Jurassic and the early Cretaceous with a Neocomian interval of reduced subsidence, (iii) after the late Albian, the basin underwent post-rift thermal subsidence (Mathieu, 1986; Roca et al., 2011), (iiii) finally from Late Cretaceous to late Oligocene the basin was inverted in response to the Pyrenees mountain belt building (Brunet, 1994; Ortiz et al., 2020). This latest phase is responsible for the creation of the Parentis field anticline. The maximum burial phase take place during Late Cretaceous time (Vermilion, pers. comm.) and the Parentis field shows 1500 meters of Tertiary sediments.

The Parentis field, an east-west anticline, (Fig. 1A) is located in the Parentis sub-basin (Ardaens, 1992; Biteau et al., 2006; Enjalbert, 1957; Mathieu, 1986; Mathieu et al., 1984; Vajk and Walton, 1956). The structural style, mostly inherited from the Lower Cretaceous, is influenced by the mobility of the Keuper salt (Trias), with simple anticlines. The maximum relief of the structure is in the eastern part of the field, while the western part shows a more moderate dip of the anticline (Fig. 1B). Seismic images show that this structure is

located directly above a Triassic saliferous bulge (Mathieu et al., 1984; Mediavilla, 1987). In addition, the major fault appears to be rooted in this level.

The reservoirs are composed of a succession of limestone and dolomite levels of Lower Aptian, Barremian, Neocomian and Upper Jurassic ages. The main cover of the reservoirs is the marly Upper Aptian. Several types of reservoirs are present, classified according to their degree of porosity and permeability. The most prolific corresponds to very porous and permeable rock in the dolomitic zones of the field. These favorable characteristics are linked to intense fracturing associated with significant dissolution (karst, very vacuolated rock, even cavernous rock, etc.) (Ardaens, 1992).

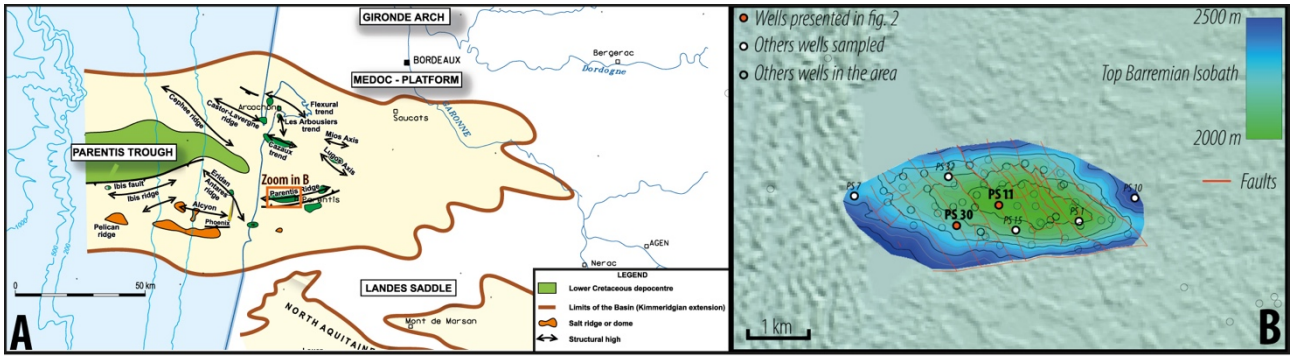

Figure 1. A) Location of the Parentis field in the Parentis Basin (modified from Biteau et al., 2006), B) Isobath of the Top Barremian (meters) with the associated faults, location of the studied wells.

Numerous hypotheses exist about the formation of this prolific reservoir, based on both dolomitization and karstification. They have been outlined in various internal ESSO-REP reports and in publications (Ardaens, 1993, 1992; Arents, 1978; Chueca, 1959; Todd, 1989). Several processes (dolomitization, karstification, faulting, compaction, oil migration) have been described, but the hierarchy of these processes and their relative contribution to the formation of the reservoir are still under discussion, and no consensus has been reached in the literature. Our study aims to characterize the establishment of these karstifications over time and understand the origin and sourcing of the dolomitization.

2 MATERIALS AND METHODS

The Parentis oil field has been studied since its discovery in 1954. A total of 122 wells have been drilled since then and many cores are available (Fig. 1B). The initial work focused on describing the core data (sedimentology, structure, karstification) from the Vermilion core storage (STC Boussens) while also examining all the thin sections (covered) available.

To understand the reservoir's formation and modification over geological time, 160 samples were collected from 7 wells, spanning from the western to the eastern part of the field. Additionnally, 140 new thin sections were prepared for optical microscopy observations and cathodoluminescence characterizations. These two methodologies enabled the construction of a paragenesis and a hierarchy of the cements and veins associated with structural features. Geochemical isotopy analysis (δ13C ‰, δ18O ‰, $^{87}Sr/^{86}Sr$) were conducted to constrain the composition and age of the parent fluids. In this paper, only the strontium isotopy will be presented, as the other geochemical analyses are still ongoing.

3 RESULTS

The first results on this study focus on two wells located in the central part of the anticline structure (Figs. 1B, 2). These results are based on different scales of description and different methods, ranging from core analysis to thin sections and from cathodoluminescence to strontium isotopy.

3.1 Core and thin section observations

The sedimentary sections (Fig. 2A) reconstructed from the original core description sheets have provided a better understanding of the distribution of lithologies and of the area of no-recovery (associated with mud loss). These sedimentary sections (Fig. 2A) synthetise lithology, sample location, areas of no-recovery, and the locations of faults and fractures from core observation, the 3D seismic model (Vermilion, pers. comm.) and the literature (Arents, 1978). The correlation between reservoirs is also indicated. Numerous occurrences of no-recovery areas are visible on the core boxes (indicated by the grey color on Fig. 2A).

The PS11 well (Fig. 2A) shows such areas in the R3 and R4 reservoirs. Where the core is available, fractures and faults are observed (between 2105 m and 2130 m in PS11, Fig. 2B-C). Faults from the 3D seismic data from Vermilion are also present in this interval. The PS30 well (Fig. 2A) also shows an area of no-recovery in the R4 and R5 reservoirs (between 2410 m and 2470 m in PS30, Fig. 2A). The 3D seismic

model shows faults in this interval. In PS30, adjacent to this fracture zone, evidence of fluid circulations is visible (Fig. 2D).

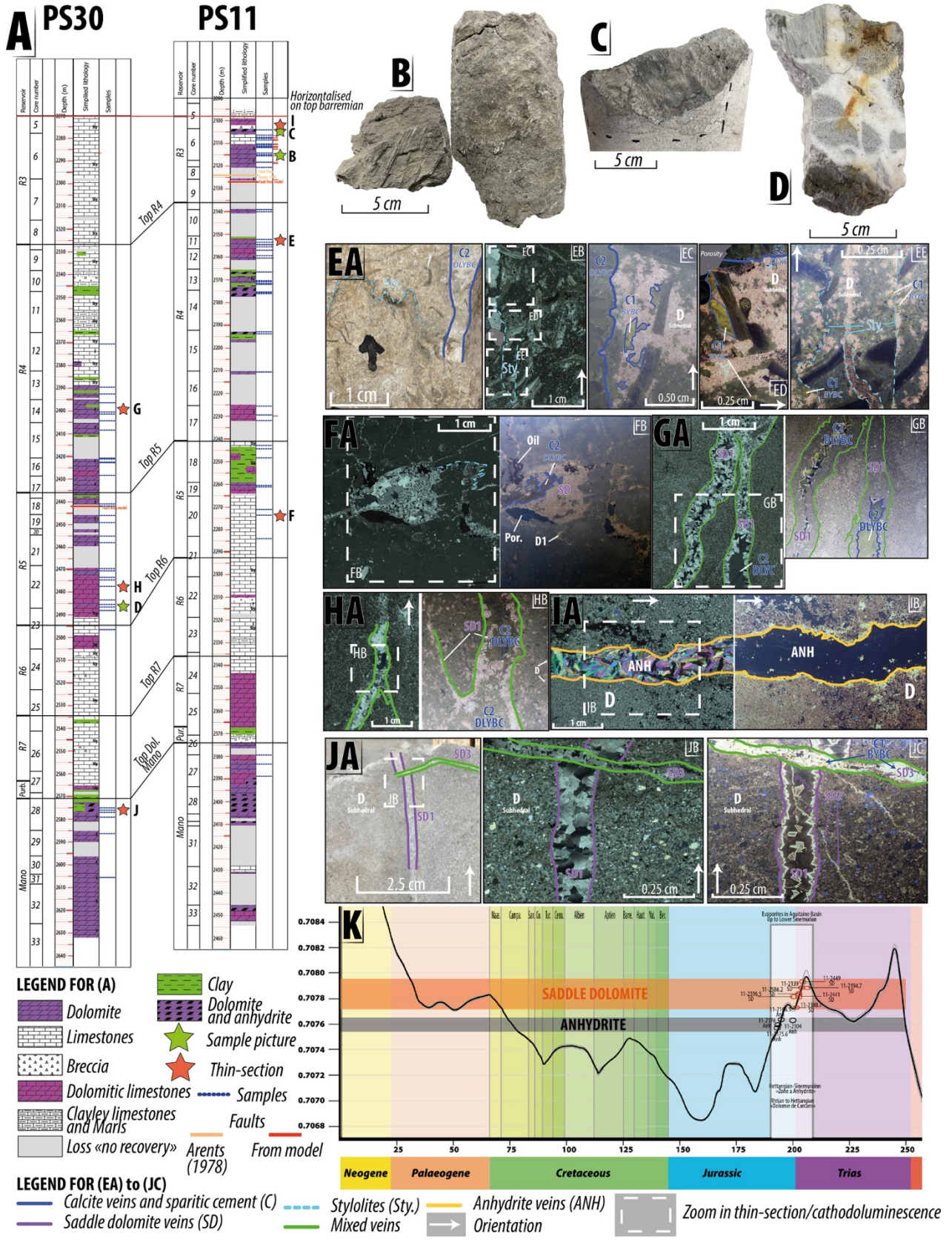

Figure 2. A) Synthetic sedimentary logs of PS11 and PS30 wells, with simplify lithologies, no-recovery, samples location, faults (from core observation, Vermilion seismic model and literature, Arents, 1978). B to D) samples, showing fault expression (striated fault) and fluid circulations with white saddle dolomite veins on cores. EA) Sample pictures showing stylolite and calcite vein. EB) Thin section (PLA) with three dotted

rectangles for EC, ED, and EE zoom, EC, ED, EE) cathodoluminescence showing dolomite (D-Subhedral), stylolite post-dolomitization and two calcite cements (C1-Bright Yellow Blocky Calcite and C2-Dull to Light Yellow Blocky Calcite). FA) Thin section (PLA) with dotted rectangles for FB. FB) Cathodoluminescence showing relation between dolomite (D1), saddle dolomite (SD), calcite (C2) and oil. GA and HA) Thin section (PLA) with dotted rectangles for GB and HB. GB and HB) Cathodoluminescence showing primary dolomite cut by two veins filled by saddle dolomite (SD1) and calcite (C2). IA) Thin section (PLA) with dotted rectangles for IB. IB) Cathodoluminescence showing primary dolomite (D) cut by anhydrite vein (ANH). JA) Sample pictures showing two crosscut veins and dotted rectangle for JB and JC. JB and JC) PLA and cathodoluminescence images, with dolomitize mixed siliciclastic-carbonate rocks with two veins of saddle dolomite (SD1 and SD3) attesting for multiple fluids circulations. K) Strontium isotopy values of saddle dolomite and anhydrite from veins (from sample collected in PS11 and PS30) on the curve modified form McArthur et al. (2012).

The areas of no-recovery appear to be linked with intervals where faults and large veins are observed. Additionally, no stratigraphic correlation exists between dolomitization and no-recovery between the PS11 and PS30 wells. No classic epigenic karstification features (such as speleothems, clay and sand karst-infill) were observed in these two wells.

In thin section and cathodoluminescence images, several minerals and cementation features were observed, reflecting the complex history of reservoir formation. The original limestones (packstone to grainstone) show dolomitization (Fig. 2EC, 2ED, 2EE 2GA, 2GB, 2HA, 2HB, 2IA, 2IB, 2JA, 2JB, 2JC) with euhedral to subhedral dolomite which may be full or partial. Several veins and geodic mineralizations were observed at sample and thin section scales (Fig. 2D to 2JC). Three major minerals are represented: saddle dolomite (SD) (Fig. 2D, 2GA, 2GB, 2 HA, 2HB, 2JA, 2JB, 2JC), anhydrite (ANH) (Figures 2IA, 2IB), and calcite (C) (Fig. 2EA, 2EB, 2EC, 2ED, 2GB, 2HB, 2JC). Saddle dolomite, with its undulatory extinction in PLA and its anhedral (non-planar) shape is known to be hydrothermal form of dolomite (Machel, 1987; Radke and Mathis, 1980). Saddle dolomite can be found with anhydrite and/or calcite (Fig. 2G). At least three generations of saddle dolomite veins are observed (Fig. 2JC). Anhydrite veins can be related linked with saddle dolomite veins or be alone (Fig. 2IA, 2IB). Calcite cements show two generations which are distinguished by their luminescence (C1 and C2), these cements can be found in veins (with saddle dolomite) (Fig. 2GB, 2JC) and filling vuggy porosity (Fig. 2EC, 2EE) in saddle dolomite or primary dolomite (Fig. 2FA, 2FB). Figure 2FA shows also oil impregnation crosscutting all the cements.

In terms of chronology, figure 2EE shows a concentration of euhedral dolomite in stylolite which occurs due to differences in solubility between calcite and dolomite. This primary dolomitization (D-Euhedral, Subhedral) predates compaction due to burial (maximum burial occurred during late Cretaceous, Vermilion Pers. Comm.; Brunet, 1994; Mathieu, 1986). Then, several veins cross the horizontal stylolites (Fig. 2EB, 2FA, 2EE) and thus postdate the compaction phase. These veins are formed by both hydrothermal (saddle dolomite) and sulphate rich (anhydrite) minerals. These veins are all located next to the fault, and the degree of veins occurrences decrease as you move away from the accidents. Oil migration could occur after all these episodes of fluids.

3.2 Strontium isotopy

Strontium isotopy has been performed on the saddle dolomite and anhydrite (veins) to identify the origin of the fluids reponsible for the large modification of the reservoir properties. Four anhydrites and seven saddle dolomites were analyzed. Anhydrite $^{87}Sr/^{86}Sr$ values shows a variability from 0.707595 ± 0.000010 to 0.707636 ± 0.000009. Saddle dolomite $^{87}Sr/^{86}Sr$ values shows a variability from 0.707732 ± 0.000009 to 0.707933 ± 0.000010. Theses values are plotted on the $^{87}Sr/^{86}Sr$ global marine signal curve from McArthur et al., (2012) (Fig. 2K). At the first order, the $^{87}Sr/^{86}Sr$ value, which reflect the age of the chemical stock (magnesium and suflur), could correspond to several geological time (Figure 2K), including Palaeogene, Upper Cretaceous and Trias-Hettangian. In the sedimentary history of the Parentis basin, no evidence of large evaporites and dolomite have been described in Paleogene and Upper cretaceous. The Triassic ("Dolomie de Carcans") and Hettangian-Sinemurian ("Zone a anhydrite") sediments are rich in magnesium (dolomite) and sulfur (anhydrite) (Fig. 2K) (Ferrer et al., 2012; Mathieu, 1986). These levels could be strong candidates for the sourcing of theses hydrothermal circulations.

4 FIRST CONCLUSIONS ON THE KARSTIFCATION/DOLOMITIZATION

Initial work on two wells in the Parentis field (PS 11 and PS 30) has revealed diagenetic transformations that could lead to reservoir modifications, i) dolomitization of the limestones (partial or full) with euhedral and subhedral dolomite, ii) compaction (stylolite), iii) faulting and fluid circulation near the fracture zones, leading to veins and geodic mineralizations (saddle dolomite, anhydrite, calcite). Several no-recovery areas were identified, all of which are located near these fracture zones. No classic epigenic karstification (speleothem, clay and sand pockets) was observed in these two wells.

The first results on $^{87}Sr/^{86}Sr$ indicate a possible Triassic/Lower Jurassic origin for the magnesium and suflur rich minerals. Anticlinal formation during Pyrenean inversion (Tertiary) helped connecting the Barremian

reservoir with the lower part of the basin through these faults. These hydrothermal fluids could have led to hypogenic karstification, responsible for these large areas of no-recovery, which are the only evidence of voids created by karstification.

These preliminary results need to be confirmed by studying the other wells mentioned and the 3D seismic data to confirm this initial hypothesis about karstification/dolomitisation in the Barremian reservoir at the Parentis field scale.

5 ACKNOWLEDGMENT

This work is being carried out under a CICo agreement between BRGM and VERMILION REP SAS. This work has benefited from state aid managed by the “Agence Nationale de la Recherche” (ANR) as part of the future investment programme for the IMAGINE project under the reference “ANR-21-ESRE-0043”. The authors and editors would like to thank also the reviewers, Michel Séranne and Jean-Jacques Biteau, who helped improving the paper.

6 REFERENCES

Ardaens, R., 1993. Champ de Parentis, Bilan des études géologiques. Rapport interne ESSO/REP.

Ardaens, R., 1992. Le champ de Parentis. Réservoir carbonaté complexe et paléokarst. Pétrole et techniques, 372, 34–42.

Arents, C., 1978. Ré-interprétation géologique du Champ de Parentis. Rapport interne ESSO/REP.

Biteau, J.-J., Le Marrec, A., Le Vot, M., Masset, J.-M., 2006. The Aquitaine basin. Petroleum Geoscience, 12, 247–273.

Bourrouilh, R., Richert, J., Zolnaï, G., 1995. The North Pyrenean Aquitaine Basin, France : Evolution and Hydrocarbons. AAPG Bull, 79, 831–853.

Brunet, M.F., 1994. Subsidence in the Parentis Basin (Aquitaine, France): Implications of the Thermal Evolution, in: Mascle, A. (Ed.), Hydrocarbon and Petroleum Geology of France. Springer, Berlin, pp. 187–198.

Chueca, A., 1959. Répartition des caractéristiques et facteurs influençant la récupération finale dans un réservoir carbonaté hétérogène. 5th World Petroleum Congress, New York, USA, paper WPC-8118.

Desegaulx, P., Brunet, M.-F., 1990. Tectonic subsidence of the Aquitaine basin since Cretaceous times. Bulletin de la Société géologique de France, 8, 295–306.

Enjalbert, H., 1957. Parentis. Revue géographique des Pyrénées et du Sud-Ouest, 28, 35–59.

Ferrer, O., Jackson, M.P.A., Roca, E., Rubinat, M., 2012. Evolution of salt structures during extension and inversion of the Offshore Parentis Basin (Eastern Bay of Biscay). Geological Society London Special Publications, 363, 361–380.

Machel, H.-G., 1987. Saddle dolomite as a by-product of chemical compaction and thermochemical sulfate reduction. Geology, 15, 936-940.

Mathieu, C., 1986. Histoire géologique du sous-bassin de Parentis. Bulletin des centres de recherches exploration-Production Elf-Aquitaine, 10, 33–47.

Mathieu, C., Modiano, T., Mure, E.P., 1984. Bassin de Parentis Synthèse géologique et géophysique, bilan pétrolier. Rapport interne Elf Aquitaine.

McArthur, J.M., Howarth, R.J., Shields, G.A., Zhou, Y., 2012. Chapter 7- Strontium isotope stratigraphy. Geologic Time Scale, 1, 211-238.

Mediavilla, F., 1987. La tectonique salifère d’Aquitaine. Le bassin de Parentis. Pétrole et techniques, 335, 35–37.

Ortiz, A., Guillocheau, F., Lasseur, E., Briais, J., Robin, C., Serrano, O., Fillon, C., 2020. Sediment routing system and sink preservation during the post-orogenic evolution of a retro-foreland basin: The case example of the North Pyrenean (Aquitaine, Bay of Biscay) Basins. Marine and Petroleum Geology, 112, 104085.

Radke, B.M., Mathis, R.L., 1980. On the Formation and Occurrence of Saddle Dolomite. Journal of Sedimentary Research, 50, 1149-1168.

Roca, E., Muñoz, J.A., Ferrer, O., Ellouz, N., 2011. The role of the Bay of Biscay Mesozoic extensional structure in the configuration of the Pyrenean orogen: Constraints from the MARCONI deep seismic reflection survey. Tectonics, 30, TC2001.

Todd, R.G., 1989. Paragenesis of the Parentis Field. Rapport interne ESSO/REP.

Vajk, R., Walton, G., 1956. Geophysical history of Parentis oil field, France. Geophysics, 21, 815–827.